

1 Optimization of a Hybrid Community District Heating System integrated with Thermal 2 Energy Storage system

3 Behrang Talebi¹, Fariborz Haghighat^{1*}, Paul Tuohy², Parham A. Mirzaei³

4 ¹ Department of Building, Civil and Environmental Engineering, Concordia University,
5 Montreal Canada, H3G 1M8

6 ² Mechanical and Aerospace Engineering, University of Strathclyde, UK

7 ³ Department of Architecture and Built Environment, University of Nottingham, UK
8

9 Abstract

10 Evidence from a various research suggests that buildings hold a vital role in climate change by
11 significantly contributing to the global energy consumption and the emission of greenhouse
12 gases. Considering the trend of higher energy consumption in the building sector, it is important
13 to influence this sector by decreasing its energy demand. District generation and cogeneration
14 systems integrated with the energy storage system have been suggested as a potential solution
15 to achieve such planned goals.

16 Unlike the older generation of the DHS, where the focus of the design was on minimizing the
17 system heat loss, in 4th generation DHS, achieving higher system efficiency is made possible
18 by picking the optimal equipment size as well as adopting the appropriate control strategy.

19 Designers have adopted different design methods for selecting the equipment size, however,
20 finding the optimal size is a challenging task. This paper reports the development of a simplified
21 methodology (dynamic optimization) for a hybrid community-district heating system (H-
22 CDHS) integrated with a thermal energy storage system by coupling the simulation and
23 optimization tools together. Two, existing and newly built communities, have been considered
24 and the results of the optimization on the equipment size of both communities have been
25 studied. The results for the newly built community is later compared with the one obtained from
26 the conventional equipment size methods whereas static optimization methods and potential
27 size reduction with the conventional method has been obtained.

28 **Keywords:** Hybrid Community-District Heating System; Thermal Storage; Multi-Objective
29 Dynamic Optimization; Load Prediction Method

30 *Corresponding Author: Fariborz.Haghighat@Concordia.ca
31
32
33

| <i>Variable</i> | <i>Description</i> | <i>Unit</i> |
|---------------------|--|-------------------|
| A | Thermal Storage Exterior Area | m^2 |
| C | Cost | £ |
| Cap_{TS} | Capacity of Thermal Storage | m^3 |
| $CP_{wt.}$ | Specific Heat of the Fluid, Water | $kJ/kg.K$ |
| E | CO ₂ Generation | $kg\ of\ CO_2$ |
| $E_{n,m}$ | Equivalent Emission Generated by Boiler n at Year m per Unit of Energy Generated | $kg.CO_2/kg.fuel$ |
| $ExCap_m$ | Extra Capacity of Boiler m | kW |
| $FC_{n,m}$ | Fuel Cost of Boiler m at Year n | £ |
| i | Annual Interest Rate | % |
| IC | Initial Cost | £ |
| IC_m | Base Cost of the Boiler m | £ |
| $IE_{Aux.}$ | Equivalent Emission Generated by Imported Energy Year m per Unit of Energy Generated | $kg.CO_2/kg.fuel$ |
| IN | Annual Income from Selling Energy to Off-Site | £ |
| LC_m | Linearized Cost of Boiler m | £/ kW |
| LC_{TS} | Linearized Cost of Thermal Storage | £/ m^3 |
| $Loop_{DN}$ | Demand Side Loop | kWh |
| M | Boiler Number | |
| N | Year Number | |
| $\square_{Ch.}$ | Charging Efficiency = 0.98 | |
| $\square_{Dis.Ch.}$ | Discharging Efficiency = 0.96 | |
| OC_{annual} | Annual Operational Cost | £ |
| $PRFF_n$ | Primary Resource Factor of the Fuel | |
| $PRFIE$ | Primary Resource Factor of the Imported Fuel | |
| PW_{oc} | Present Worth of Operational Cost | £ |
| $Q_{BLDG(t)}$ | Energy Required by the Buildings, Users, at Time t | kWh |
| $Q_{Gen(t,n)}$ | Energy Generated by Boiler n at Time t | kWh |
| $Q_{Losses(t)}$ | Energy Lost Through Distribution Network at Time t | kWh |
| $Q_{Net(t)}$ | Net Energy Required by the Network at Time t | kWh |
| $Q_{TSCh(t)}$ | Energy Sent to Thermal Storage at Time t | kWh |
| $Q_{TSDis.Ch(t)}$ | Energy Discharged From Thermal Storage at Time t | kWh |
| $Q_{TS.loss(t)}$ | Energy Loss of the Thermal Storage at Time t | kWh |
| $T_{OA(t)}$ | Outdoor Temp. at Time t | °C |
| $T_{TS(t)}$ | Thermal Storage Temp. at Time t | °C |
| U | Overall Heat Transfer Coefficient of Thermal Storage | $W/(m^2.K)$ |
| V | Volume of the Thermal Storage | m^3 |
| $V_{Aux.}$ | Amount of Imported Fuel Used to Generate a kWh of Energy | $kg.fuel/kWh$ |
| $V_{n,m}$ | Amount of Fuel Used to Generate a kWh of Energy | $kg.fuel/kWh$ |
| $\rho_{wt.}$ | Density of the Fluid, Water | kg/m^3 |

35

36

37

38

39

40

Abbreviation

| Abbreviation | Description |
|--------------|--|
| H-CDHS | Hybrid Community District Heating System |
| DHS | District Heating System |
| DHW | Domestic Hot Water |
| NTHU | Non-Typical High Usage |
| NTMU | Non-Typical Medium Usage |
| NTLU | Non-Typical Low Usage |
| TTCU | Typical Thermostat Control Usage |
| TMY | Typical Meteorological Year |
| MLCP | Mixed Linear Complementarity Programing |
| LCC | Life Cycle Cost |

41

42

43

Major TRNSYS Components

| Type No. | Name | Representing |
|----------|---|--|
| 700 | Simple Boiler with Efficiency Input (Modified) | <i>Biomass Boiler</i> |
| 659 | Auxiliary Fluid Heater with Proportional Control (Proportional Boiler) | <i>Auxiliary Boiler</i> |
| . | Equa. 2 | <i>Boiler House Controller</i> |
| . | Equa. 3 | <i>Network Controller</i> |
| 534 | Vertically Cylindrical Storage Tank with Optional Immersed Heat Exchanger | <i>Thermal Storage</i> |
| 512 | Sensible Heat Exchanger With Hot-Side Modulation | |
| 940 | Tank-less Water Heater | |
| 977 | Variable Speed Pump | <i>Circulation Pump</i> |
| 604a | Bi-Directional, Noded Pipe with Wall & Insulation Mass | |
| 952 | Buried Single Pipe | <i>Under Ground Distribution Network</i> |
| 682 | Load Imposed on a Liquid Stream | |

44

45

46

47

48

49

50

51

52

53

54 1. Introduction

55 As a major energy consumer, the building sector accounts for about 40% of the total
56 energy consumption in North America and Europe, respectively [1]. Various countries
57 prioritize the implementation of energy enhancement strategies in this sector to respect the Paris
58 Climate Accord, COP21[2]. Such strategies have been applied at various levels, including
59 energy production, conversion, and user-demand, but the most effective solution touches the
60 higher level known as energy management [3].

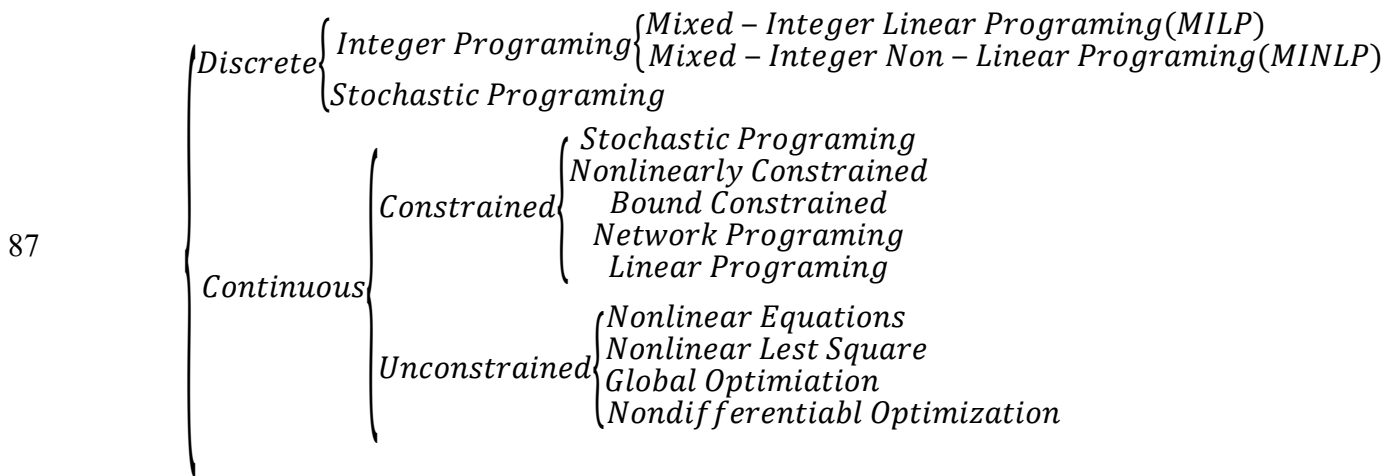
61 A Hybrid¹ Community-District Heating System (H-CDHS) is a unique type of energy
62 management integrating thermal storage within its multi-source energy fed system. Two types
63 of renewable sources exist in terms of availability a) intermittent sources such as wind and
64 solar, and b) non-intermittent sources such as biomass and geothermal. For the intermittent
65 sources, thermal storage can regulate the demand which could decrease the dependency on non-
66 renewable sources. However, for non-intermittent sources, thermal storage can appreciably
67 improve the system performance and its efficiency in other ways such as peak demand shaving.
68 [4].

69 The major design issue of the older district heating system (DHS) generations (1st to 3rd
70 generation) was mainly high heat loss in the distribution network due to the high-temperature
71 media (100°C and more) [5, 6]. In this regard, the optimization focus was on enhancing the
72 system efficiency by controlling the heat loss from the system and subsequently, improving the
73 system efficiency. As a result, most optimization studies have focused on minimizing the
74 system heat loss. However, the new generation DHS (4th generation) operates at a lower
75 temperature (50-60°C), and hence achieving higher system efficiency is possible by adopting

¹ The term hybrid, represent the use of multiple energy generation sources, renewable source (Biomass Boiler) and non-renewable source (Gas Boiler), used in the boiler house.

76 appropriate control strategies and also through optimization of the equipment size [7, 8]. Note
 77 that, designing the 4th generation DHS based on the conventional design method, sizing the
 78 equipment based on the peak demand load, could lead to oversizing of the equipment and low
 79 system efficiency. Therefore, the adoption of an optimal approach (for cost, energy and
 80 environmental impact) to enhance the efficiency of the DHS while designing the 4th generation
 81 DHS became a standard practice among designers.

82 Different optimization methods have been developed to improve H-CDHS efficiency
 83 and to reduce the system's emission footprint and the overall cost [4, 9]. Among the existing
 84 methods, mathematical methods based on continuous or discrete variables (**Figure 1**) [3, 10-
 85 12], generic algorithms [3, 13-15] and neural networks systems are the most implemented
 86 techniques for optimizing the DHS efficiency.



88 **Figure 1:** Summary of mathematical based optimization approaches

89 **1.1. Static and Dynamic Optimization**

90
 91 Besides the mathematical approaches (as shown in **Figure 1**) adopted to formulate the
 92 optimization process, the optimization methods could be categorized either as static or dynamic
 93 optimization based on the dependency of the decision-making process with respect to time. In

94 static optimization, the optimization time period remains the same for each iteration and the
95 optimal solution is selected for a particular point of time within the given time period. In other
96 words, in each iteration, regardless of any change in the optimization variables, the optimal
97 solution is always at the same time. For example, static optimization obtains the optimal size
98 of the equipment based only on the annual peak demand load. While in dynamic optimization,
99 the optimization time horizon is split into a set of smaller time periods and the solution for each
100 period affects the future solutions and possibilities. As a result, the optimizing agent takes into
101 account this effect in the decision-making process.

102 Even though there is a scientific consensus on the mathematical definition of the static
103 and dynamic optimization processes, there are many ongoing debates as to which type of
104 optimization method should be used when it comes to use of the commercial energy simulation
105 and optimization tools. Since similar simulation output could be obtained from all these
106 commercial methods (e.g. energy demand profile), the interaction between the simulation and
107 optimization tools can be used to identify the optimization type (static or dynamic
108 optimization). For instance, in static optimization, the district component and the interaction
109 between them are modeled either using the user-defined code or commercial simulation
110 software [19, 20] in order to find the optimal size of the DHSs' equipment [11, 16-18].
111 Subsequently, the energy simulation is performed exclusively from the optimization process
112 and a set of unique solution is obtained per simulation. In other words, the optimization
113 population is generated by simulating the model over the simulation time period under different
114 scenarios (optimizations variables) and the unique solution is obtained based on the objective
115 function (i.e. cost and emission) under each scenario. Later on, the optimization tools use the
116 unique solutions as an optimization population to find the optimized value of the objective
117 function. It is worth mentioning that all unique solutions obtained from static optimization are
118 for the same exact point of time (e.g. the peak demand time). By using the non-interactive

119 model, i.e., separate simulation and optimization model (static model), there exists a higher
120 probability of decreasing the effectiveness of the optimization tool towards predicting the
121 optimal size of the equipment [16].

122 On the other hand, in dynamic optimization, instead of generating the optimization
123 population by simulating the model for different scenarios, the optimization and simulation are
124 carried out simultaneously. By simultaneously performing the optimization and simulation, not
125 only a more comprehensive spectrum of the solution is generated as an optimization population,
126 but also the generated off-spring population reflect the effects of previous hours. Due to the
127 complexity of coupling the simulation and optimization tool in dynamic optimization, several
128 research works focused on the dynamic optimization using user-defined codes for system
129 modeling² [12, 21-23].

130 Since the dynamic optimization of the system using the detailed user-defined codes is
131 computationally expensive, and in many cases not feasible, different simplification approaches
132 have been adopted to decrease the computational time. These approaches resulted in a
133 simplification of the district energy model³, using the reduced input file and the representative
134 weather or demand file for the design period instead of using the whole year profile, or the
135 combination of two. Considering the above-said research gap, the main objective of this study
136 is to develop a dynamic optimization platform that could explore the optimal equipment size
137 using the detailed demand profile in a timely manner. The developed model predicts the detailed
138 demand profile of the DHS and uses them along with detailed energy model of the DHS and
139 the equipment, and the interaction between them to dynamically optimize the entire system.
140 Subsequently, the optimal size of the equipment is obtained. The size of the equipment obtained

² Modeling the district components and the interaction between them.

³ Represent the components and the interaction between them with a simplified equation

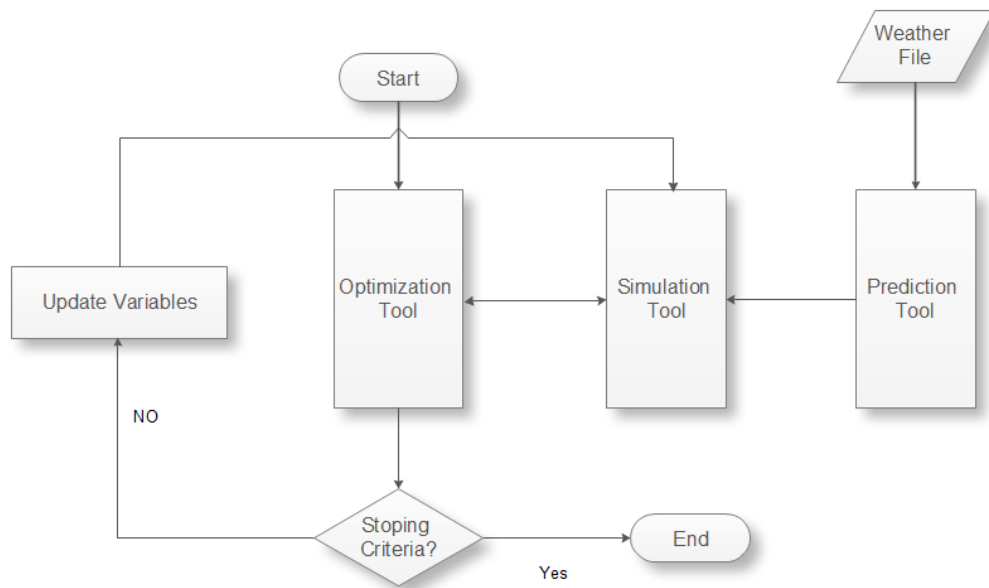
141 from the model is later compared with the one obtained from the conventional method (design
142 day method), as well as using a static optimization tool, (Biomass optimization tool). In this
143 regard, data from an existing H-CDHS with an integrated thermal energy storage system is used
144 to optimize its boiler house to minimize its overall cost and CO₂ emission.

145

146 2. Methodology

147 In this study, a mid-size H-CDHS considered earlier was used [24, 26]. The selected
148 community is located in Cambuslang, Scotland and consists of 3 different types of residential
149 buildings, newly renovated towers, newly built duplex detached houses and 4-story terrace
150 buildings, with a total of 640+ units. Multiple energy sources such as gas and wood pellets were
151 used to provide the required energy to meet the heating and DHW demands. A well-insulated
152 underground pipe network with a total length of 6 km (supply and return) is used to distribute
153 the energy between the generation and consumers. TRNSYS was used as the simulation
154 platform to define the relationship between various system components and to couple the
155 prediction and optimization tools. Also, a previously developed simplified load prediction
156 model by the authors was used to dynamically predict the system demand load [24] . Results
157 obtained from the prediction tool (User Code) demand profile of the system, were fed as input
158 to the TRNSYS file in the text format. Adopting the predicted demand profile, TRNSYS model
159 determines the load required to be generated by the boiler house or to be stored in the thermal
160 storage by comparing the available stored energy and the predicted demand load.. Knowing the
161 net demand profile and the partial efficiency profile of each boiler, TRNSYS determines the
162 type and amount of the fuel required to offset the remaining demand. In the next step, the type
163 and amount of fuel as well required size of boilers and thermal storage are sent to the
164 optimization tool (GenOpt.) in form of an input file. Considering all the different possibilities,

165 the optimization tool determines the optimal size of the equipment and overwrites the
166 equipment size in the simulation tool, [Figure 2](#).



167

168 **Figure 2:** Prediction, Simulation, and Optimization Process Flowchart

169 2.1. Load Prediction

170 To optimize an H-CDHS, the first step is to predict the hourly energy demand profile of
171 the entire H-CDHS, which includes the energy consumption and its corresponding losses. In
172 general, there are three different techniques to obtain a community's energy demand profile:
173 direct measurement, a comprehensive energy simulation tool used when data is not available,
174 and simplified prediction methods in cases with high computational costs.

175 In this study, a simplified four-step procedure developed was used to predict the
176 communities' energy demand profile [26]. The proposed model, by studying the energy
177 behavior of the users, first, cluster the users into different groups, based on their energy
178 consumption behavior. After segmenting the units among different clusters, the reference
179 building for each cluster was obtained. In third step, using the energy consumption behavior of
180 the reference building, the MLR model for each cluster was trained and used to predict the
181 energy demand profile of the remaining unit within that cluster. The accuracy of the proposed

182 procedure was validated using two different approaches, using both an inter-model comparison,
183 and comparing with measured data [26]. Using the validated model, the community demand
184 profile was predicted for two different scenarios:

- 185 • **Scenario I:** Optimizing the district's existing condition by considering users'
186 demographic distribution regarding energy consumption habits.
- 187 • **Scenario II:** Optimizing the community as a newly built district by using design
188 criteria and thermostat control to simulate all users' energy behavior.

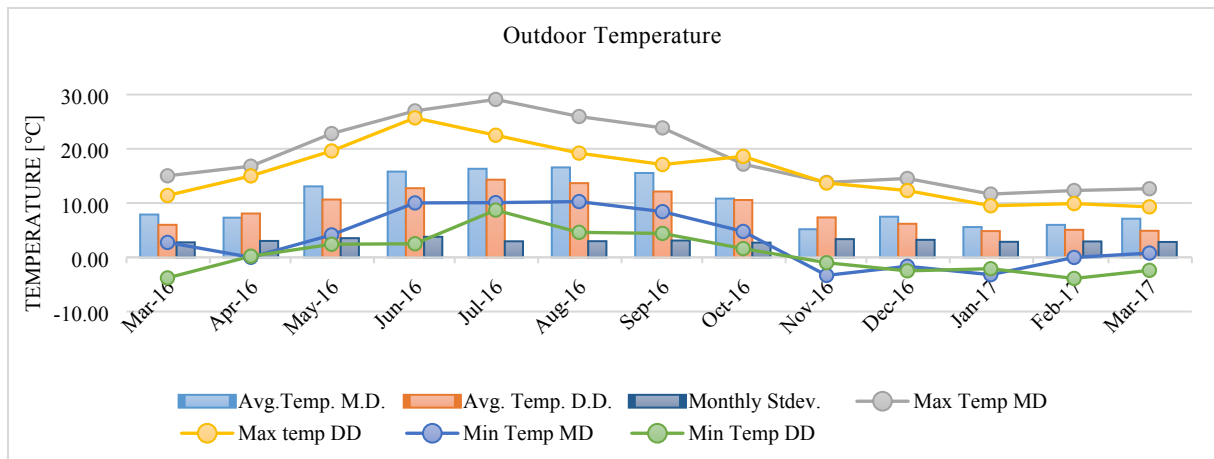
189 Before performing the above-said optimization scenarios, in the first step, the
190 community demand profile was predicted. In order to predict the community demand profile,
191 occupants were divided into four different groups based on their energy consumption habits⁴.
192 The definition of each group and its contribution to the total population presented in more
193 detailed in [26]. Once these groups' energy consumption habits were available, the prediction
194 model was trained using the proportion of each group within the community.

195 In the **Scenario I**, the proportion of the different occupants' type within the community
196 remained constant and the results served as a basis of comparison for the optimization process.
197 Leaving occupants' demographic distribution untouched, the district energy demand profile for
198 **Scenario I** was predicted using the on-site weather data. Then using the on-site measured data
199 the accuracy of the energy simulation tools' (TRNSYS) was validated, as the all on-site
200 measured data correspond with this scenario. As a result, **Scenario I** compares the effect of
201 optimized equipment size and control strategy on energy consumption pattern of the existing
202 community, its CO₂ emission, and cost.

⁴(*Non-Typical High Usage (NTHU)*, *Non-Typical Medium Usage (NTMU)*), *Non-Typical Low Usage (NTLU)* and *Typical Thermostat Control Usage (TTCU)*) [26]

203 Conversely, in *Scenario II*, due to non-availability of data regarding the real time
204 weather and occupancy condition, both weather file and occupants' demographic distribution
205 were replaced by the design condition. Hence in this scenario, the TMY3 weather file was used
206 as a weather input data and, *Typical Thermostat Control Usage* (TTCU) profile was used as an
207 occupancy profile. Note that the main difference between two scenarios is the energy behavior
208 of the users. In newly built communities, due to unknown energy consumption profile of the
209 users, the energy demand profile of the community was obtained based on the predefined
210 schedules and the minimum temperature mandated by codes. However, in existing
211 communities, using the same procedure results in over estimating the energy consumption of
212 the community. In order to compare the effect of difference in energy demand profile on the
213 equipment size, boiler house under both scenarios has been sized and compared with each other.
214 As a result, in the first scenario, the existing community was sized by clustering the users and
215 adopting the actual energy behavior of them. However, in *Scenario II*, equipment has been sized
216 using the energy behavioral schedules and temperature mandated by codes, and subsequently
217 the obtained results were compared with the conventional method as well as static optimization
218 methods. Comparing the TMY3 file with the onsite measured weather data file used for
219 validating the model shows the average outdoor temperature of 9.3°C and 10.8°C, and the
220 minimum outdoor temperature of -3.9°C and -3.3 °C for TMY3 and onsite measured data,
221 respectively. Comparing the TMY3 average and minimum temperature, higher total load and
222 peak demand load are expected for both scenarios.

223 After obtaining both scenarios' typical usage behavior, a prediction model was trained
224 based on the fraction of each community group's data. **Figure 3**, shows the design weather
225 data, TMY3, and onsite measured weather data, while Figure 4 shows the demand heating
226 profile for these two scenarios.

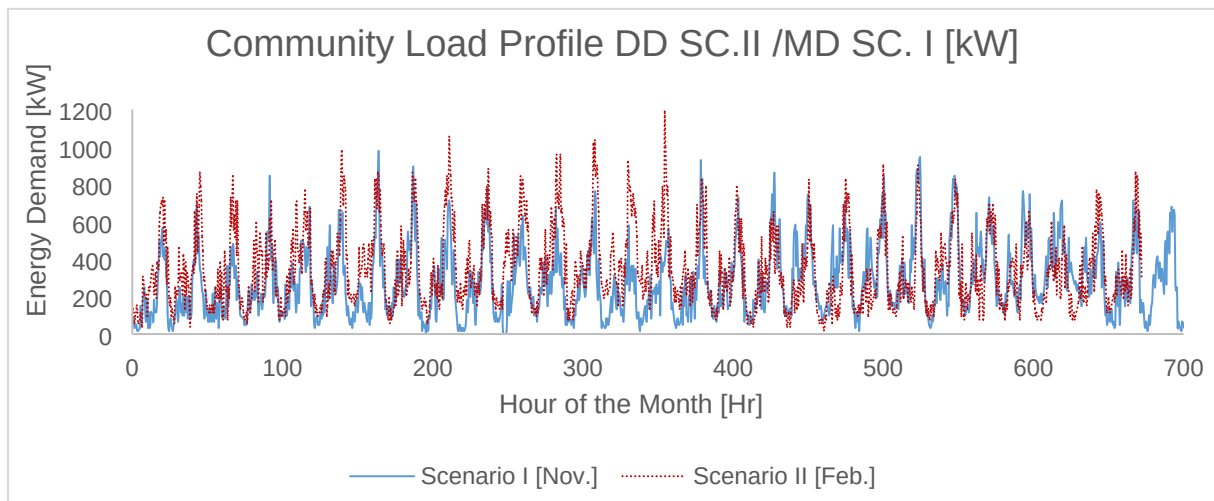


227

228

Figure 3: Outdoor weather data (MD: Measured Data and DD: Design Data)

229



230

Figure 4: Predicted Demand Profile for *Scenario I* (November) & *Scenario II* (February)

231

232

233

Figure 4 shows the heating demand profile of *Scenario I & II* for the month when the peak demand load occurred. The inference from the figure is that the peak-heating demand load is 977.3 kW (2.8 % higher compared to the onsite measured data) in the *Scenario I*, and 1189 kW (25.1 % higher compared to the onsite measured data) for *scenario II*. Note that, in *Scenario II*, the entire community was simulated assuming all units were conditioned using the thermostat control (TTCU). It is also important to note that domestic hot water usage was constant for both scenarios. Therefore, the 25.1% increase in peak demand load was associated only with the community's higher heating demand.

240

241 2.2. Energy Modelling

242 TRNSYS was used to predict the district energy demand profile and the interaction between its
243 different components. To represent components, such as biomass boilers and building stock,
244 existing types in TRNSYS were modified. In general, TRNSYS has three major loops:

245 2.2.1. Generation Loop

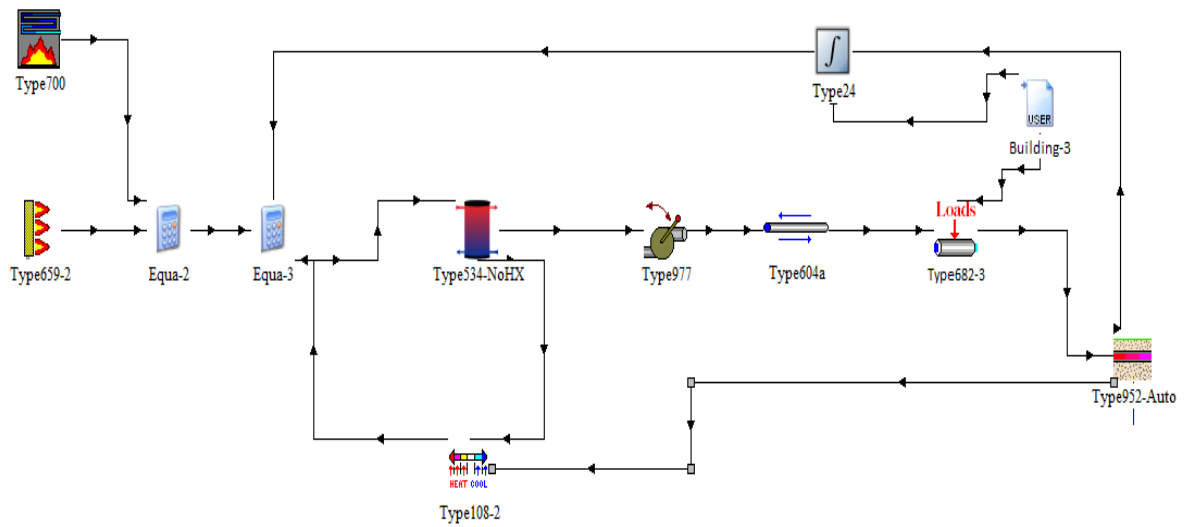
246 The first loop (generation loop) consists of the auxiliary gas, biomass boilers, a
247 controller, and a heat exchanger, which feeds energy into the system, as shown in [Figure 5](#) and
248 [Figure 6](#). Since no specific biomass boiler type exists in TRNSYS, *Type 700* was modified to
249 represent the biomass boiler by adjusting its efficiency, partial efficiency, and the control signal.
250 After adjusting the boilers' type, two controllers were assigned to the generation loop to adjust
251 the flow pattern between the generation/consumption loops and the storage loop. The first
252 controller compared the network's predicted demand load with the total capacity of the boiler
253 house and the need for the thermal energy storage system as a backup. The second controller
254 decides which boiler (biomass or gas) should operate to provide the required energy.

255 2.2.2. Consumption Loop

256 The consumption loop was constructed with *Type 682*, which represents the demand
257 profile of all units, ([Figure 4](#)). This *Type* reads the predicted demand profile through an external
258 link. The distribution network heat loss was modeled using *Type 952*.

259 2.2.3. Storage Loop

260 The storage loop was formed with two different configurations. The first configuration
261 was modeled by simultaneously charging and discharging the thermal storage as shown in
262 [Figure 5](#).



263

264

Figure 5: Simultaneous charging and discharging configuration

265

266

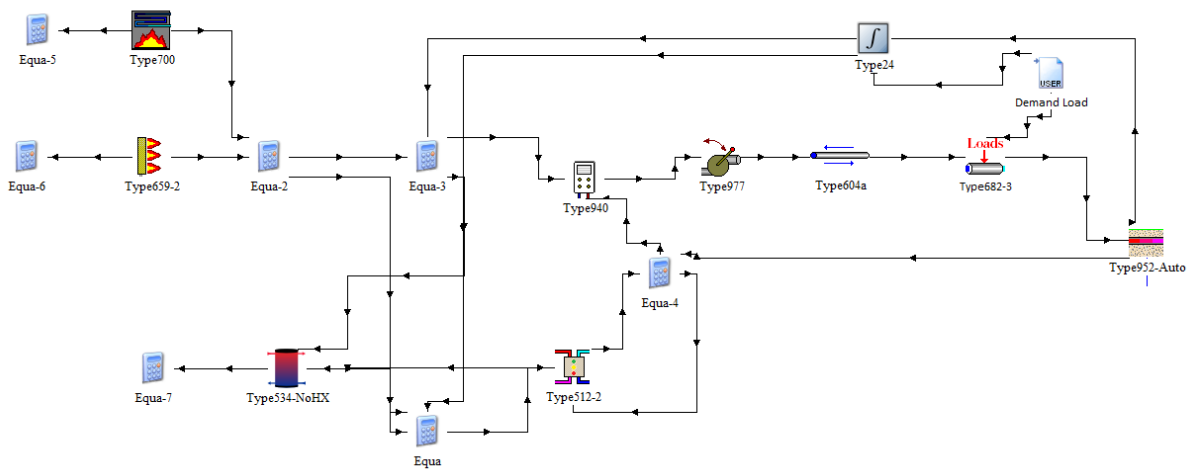
267

268

269

270

In other words, both the boiler house and distribution network was connected to the thermal energy storage system. While the boiler house provided energy to the thermal storage system, the latter supplied the energy to the distribution network. The second configuration was modeled using a step-wise energy storing procedure (Figure 6). In this configuration, a controller monitored the direction to the thermal storage tank (either charged or discharged).



271

272

Figure 6: Step-wise charging and discharging configuration

273 By comparing the preliminary results obtained from the total heat loss of the two
274 configurations (simultaneous and stepwise), it is inferred that the step-wise charging and
275 discharging configuration had the lower heat loss than simultaneous charging/discharging
276 configuration due to thermal system storage size and flow direction. Also, the step-wise
277 charging and discharging configuration has a higher overall energy efficiency compared with
278 the simultaneous charging/discharging due to on/off frequency of the generation loop in this
279 configuration (refer [Figure 5](#) & [Figure 6](#)). More detailed explanations regarding the efficiency
280 of the system are given in the following sections. As a result, the second configuration is used
281 as a base for optimization.

282 **2.3. Optimization Formulation**

283
284 As mentioned earlier in literature review, the main focus of this study is to optimize the size of
285 the equipment in a dynamic manner. Existing method, such as using TRNSYS type 56 or Energy plus
286 optimization function (both using GenOpt.) result in static optimization of the model. In both cases, the
287 energy simulation is performed exclusively from the optimization process. Subsequently, an
288 optimization population is generated by simulating the model over the simulation time period under
289 different scenarios (optimizations variables) and the unique solution is obtained based on the objective
290 function (i.e. cost and emission) for each scenario. The existing method is effective for optimization of
291 the component which is not sensitive to previous time steps, such as boilers and earlier generation of the
292 district system which does not have a thermal storage system. However, for components such as thermal
293 storage systems which are sensitive to the amount of excessive/lacking energy at previous time steps,
294 this method cannot result in finding the optimized solution. In this aspect, the existing method has been
295 modified to perform the dynamic optimization.

296 For the design stage, a dynamic multi-objective optimization method was chosen to size the
297 main components of the district network boiler house for the two defined scenarios. The model
298 was based on Mixed Linear Complementarity Problem (MLCP) to minimize the objective

299 functions, life cycle cost (LCC) and CO₂ emission. The optimization analysis focused on the
 300 on-site heat generation, but the option of purchasing auxiliary heating energy was also
 301 considered. This is because the primary goal of optimization is to size the main components of
 302 the boiler house to minimize the investment and operational costs over a thirty-year cycle. To
 303 account for the effects of short-term load fluctuations on the components' optimal size, the
 304 optimization was conducted daily with an hourly temporal resolution. To improve model
 305 accuracy, other input data and model characteristics, including minimum and maximum output
 306 level constraints, and partial load efficiencies, were defined on an hourly basis. The system
 307 operational and fuel costs were also considered.

308 A controller type (*Equa.-3* in **Figure 6**) was developed to compare the energy generated
 309 at each time-step with that in the boiler house (*Equa.-2* in **Figure 6**) in accordance with the
 310 network demand load (*Type 24*)⁵ and flow direction. By comparing the demand load and
 311 generation capacity, controller fed the network first and then it decides whether to use the
 312 disparity between generation and demand to charge or discharge the thermal storage system,
 313 [Equation 1-4](#). This implies that the controller regulates flow direction based on the general heat
 314 balance equation, while other constraints (such as minimum operative temperature ($T_{TS(t)}$))
 315 were set for the thermal storage ([Equation 9](#)) to ensure a minimum required temperature for
 316 DHW usage:

$$317 \quad \sum_{n=1}^N Q_{Gen(t,n)} + Q_{TSCh.(t)} - Q_{TSDis.Ch.(t)} \geq Q_{Net(t)} \quad (1)$$

$$318 \quad Q_{Net(t)} = Q_{BLDG(t)} + Q_{Losses(t)} \quad (2)$$

319 If

$$320 \quad Q_{Gen(t,n)} \geq Q_{Net(t)} \rightarrow \begin{cases} Q_{Net(t)} \rightarrow Loop_{DN(t)} \\ Q_{Gen(t)} - Q_{Net(t)} \rightarrow Q_{TSCh.(t)} \end{cases} \quad (3)$$

321

⁵ Type 24 is the sum of heat loss of underground pipes obtained from Type 952 and the predicted demand load of the buildings obtained from the simplified method and fed to the TRNSYS model as an external user file (Demand Load)

$$322 \quad Q_{Gen(t,n)} < Q_{Net(t)} \rightarrow \begin{cases} Q_{Gen(t)} \rightarrow Loop_{DN(t)} \\ Q_{TS_{Dis.Ch.}(t)} \rightarrow Q_{Net(t)} - Q_{Gen(t)} \rightarrow Loop_{DN(t)} \end{cases} \quad (4)$$

323

324 The equations used for modeling thermal storage, such as total energy at different time-steps
325 and boundary conditions applied to it, are as follows:

$$326 \quad Q_{TS(t)} = Q_{TS(t-1)} + Q_{TS_{Ch.}(t)} \cdot \eta_{Ch.} - Q_{TS_{loss}(t)} - \left(\frac{Q_{TS_{Dis.Ch.}(t)}}{\eta_{Dis.Ch.}} \right) \quad (5)$$

$$327 \quad Q_{TS(t)} \geq 0 \quad (6)$$

$$328 \quad Q_{TS_{loss}(t)} = (T_{TS(t)} - T_{OA(t)}) \cdot U \cdot A \quad (7)$$

$$329 \quad T_{TS(t)} = T_{TS(t-1)} - \left(\frac{Q_{TS_{Dis.Ch.}(t)} / \eta_{Dis.Ch.}}{V \cdot C_{p_{wt.}} \cdot \rho_{wt.}} \right) + \left(\frac{Q_{TS_{Ch.}(t)} \cdot \eta_{Ch.}}{V \cdot C_{p_{wt.}} \cdot \rho_{wt.}} \right) \quad (8)$$

$$330 \quad T_{TS(t)} \geq 70^\circ C \quad (9)$$

331 After setting up the controllers, the optimization objective function (Equation 10) was
332 set up with the aim of optimizing the size of the biomass boiler(s) and thermal storage system,
333 and minimizing the current net cost and CO₂ emissions:

$$334 \quad \text{Min}\{Obj(C, E)\} \quad (10)$$

335 where C and E are the cost and emission objectives. To make the objective function linear and
336 to simplify it from 2D to 1D, the optimization of was performed using the equation below:

$$337 \quad Obj(C, E) = \alpha \cdot C / C_0 + \beta \cdot E / E_0 \quad (11)$$

338 where α and β are the cost and emission importance factor in the final objective function. These
339 factors were obtained based on the requirements/needs of the management board. Based on the
340 discussion with the community management office, the value of α and β was considered as 0.75
341 and 0.25, respectively. The cost associated function considers the entire C-DHS initial cost in
342 addition to the present worth of the life cycle operational cost. To define the initial cost
343 (Equation 12), the main boiler house equipment was divided into two modular modifiable parts
344 (boilers and thermal storage system) and fixed non-modifiable equipment (pumps and

345 underground distribution pipelines). Note that, only the modular modifiable equipment cost was
 346 considered in the initial cost function and the initial cost of fixed non-modifiable equipment
 347 was excluded, as it remains constant regardless of the size of the modifiable equipment. For
 348 operational costs (Equation 13), the present fuel cost, the selling price of energy, and the buyout
 349 price of energy for surrounding houses for a 30-year period were considered using present
 350 worth method⁶.

$$351 \quad IC = \left(\sum_{m=1}^N (IC_m + LC_m \cdot ExCap_m) \right) + LC_{TS} \cdot Cap_{TS} (12)$$

352 where IC is the linearized initial cost of the boiler house, ‘ n ’ is the number of years, FC is the
 353 fuel costs of different boilers; ‘ m ’ is the boiler number, IN is the annual income from selling
 354 heat to off-site users and E_{tax} is the energy taxes. The initial investment cost includes the fixed
 355 and proportional variable expenses. The fixed component included the market value of the
 356 smallest size of the equipment available on the market, LC_m , while the proportional cost was
 357 determined by linearizing the extra cost associated with the higher capacity of the equipment,
 358 $LC_m \cdot ExCap_m$. Hereafter, in the text, IC_m and $LC_m \cdot ExCap_m$ are presented as A and BX,
 359 respectively.

$$360 \quad OC = \left(\sum_{n=1}^N \sum_{m=1}^M FC_{n,m} \cdot (1+i)^{-n} \right) - \left(\sum_{n=1}^N IN \cdot (1+i)^{-n} \right) + \left(\sum_{n=1}^N \sum_{m=1}^M E_{tax,n,m} \cdot (1+i)^{-n} \right)^7 (13)$$

361 The cost function (C) is the summation of the initial and operational cost, (Equation 14).

$$362 \quad C = IC + OC \quad (14)$$

⁶ $PW_{OC} = OC_{annual} \cdot \left(\frac{(1+i)^n - 1}{i \cdot (1+i)^n} \right)$ where i and n are the annual interest rate and year number, respectively, and OC_{annual} is the annual operation cost.

⁷ The energy discount rate (i) for Scotland is 0.9%

363 The second objective function is defined to minimize the total CO₂ emission. The
 364 emission associated function was calculated using the following equation:

$$365 \quad E = \sum_{n=1}^N \sum_{m=1}^M (E_{n,m} \cdot V_{n,m} \cdot PRFE_n + IE_{Aux} \cdot V_{Aux} \cdot PRFIE) \quad (15)$$

366 where $E_{n,m}$ represents the fuel emissions (kg.CO₂/kg.fuel) used for each boiler (n) in a year (m) of
 367 the operation; IE_{Aux} is the emission of the imported energy fed to the system from outside in
 368 year, (m,) of the operation (kg CO₂/kg fuel); $PRFE_n$ is the primary resource factor of the fuel; and
 369 $V_{n,m}$ is the fuel volume used in each month ‘m’ by the boiler ‘n’ . While calculating the costs,
 370 the wood price was discounted in order to take into account the government incentive on the
 371 price of wood pellets to encourage the small community to use biomass boilers. Note that values
 372 of the primary energy factor for the wood pellets (PRFE) is 1.26 and for the natural gas (PRFIE)
 373 is 1.2. [27]

374 To optimize the equipment size and to further minimize the overall costs, CO₂ emissions
 375 over the life cycle, the first step is to define the price and emissions level for the different type
 376 of fuel. **Table 1** represents the cost and CO₂ values for wood pellets and natural gas as the main
 377 fuel type for the chosen district. **Table 2** gives the initial cost of the major equipment.

378 **Table 1:** Energy cost & emission for different fuel types

| | Emission [kg CO ₂ /kWh] | £/kWh |
|---------------------|------------------------------------|-------|
| Wood Pellets | 0.039 | 0.061 |
| Natural Gas | 0.203 | 0.046 |
| Buyout | NA | 0.12 |

379
380

Table 2: Investment costs

| | Fixed £ [A] | £/kW [BX] | £/m ³ |
|-----------------------------|-------------|-----------|------------------|
| Wood Pellets Boiler | 125,000 | 362* | NA |
| Gas Fired Boiler | 132,000 | 180** | NA |
| Wood Pellets Storage | NA | NA | 670 |
| Thermal Storage | NA | NA | 1,100 |

All costs are presented in A+BX; (refer Equation.12)

Installation and other costs were added separately

* The linearized part was added after first 250 kW

** The linearized part was added after first 200 kW

381 **3. Results**

382 As mentioned in Section 2.1, two different load scenarios were defined and served as a
383 basis of comparison within existing communities (*Scenario I*) or newly built communities
384 (*Scenario II*). Using the load demand profile for each scenario, the optimization process was
385 applied separately, and the equipment's optimal size was determined.

386 **3.1. Scenario I (Existing Community):**

387 The *Scenario I* was defined based on the current situation of the H-CDHS regarding
388 occupants' behavior. By keeping a similar occupancy distribution to that of a real case one, the
389 potential annual cost saving and CO₂ emission of the district over its life cycle was determined
390 using the optimal equipment size and flow control (Table 3).

391

392 **Table 3: Scenario I: Optimization results**

| Parameters | Existing Situation | Scenario I |
|--|--------------------|------------|
| Peak Heating Load (kW) | 1100 | 978 |
| Biomass Boiler (kW) | 870 | 477 |
| Auxiliary Boiler (kW) | 1300 | 609 |
| Thermal Storage (m ³) | 50 | 16.3 |
| Biomass Boiler Size Compared to the Peak Load (%) | 79.1 | 49 |
| Coverage Percentage by Biomass and Thermal Storage (%) | -- | 95 |

393

394 The optimization results for this scenario shows a significant reduction in boiler
395 capacities (45% for Biomass boiler and 53% for the auxiliary boiler) compared to the existing

396 situation. Considering that only one boiler operates at a time, this fact only achieved by utilizing
 397 a thermal storage system, which balances the demand and supply heat between the generation
 398 and consumption loops.

399 Comparing the optimized model results with field measurements show a dramatic drop
 400 in CO₂ emission (171.9 tons of CO₂ /year or 23%), as well as a considerable reduction in the
 401 total cost of the system (79,056 £/year or 17.6%). The cost and CO₂ reductions are partially due
 402 to the lower efficiency of the oversized equipment working at a partial load while other parts
 403 can be associated to the non-optimal control strategy of the system and missing thermal storage.

404 Since specific weather data and occupants' behavior was considered in the *Scenario I*
 405 (2016-17), the demand energy load of the community could change anytime based on the
 406 number of tenants or weather conditions. Consequently, after optimizing the system and
 407 determining the optimal equipment size, the sensitivity of the design to any change in
 408 community demand load due to change in the users' demographic distribution was determined.
 409 To do that, two new cases (*High and Low Usage*) were defined. These newly defined cases
 410 included a change in the fraction of occupants' types⁸ in the community compared with the
 411 existing condition obtained from clustering results. In the *High Usage Case*, the fraction of
 412 NTLU and NTMU users dropped, were added to the NTHU and TTCU users to represent a
 413 higher demand load, see Table 4. In the *Low Usage Case*, the number of NTHU users dropped,
 414 was added to the lower energy consumers such as NTLU and NTMU, see [Table 4](#).

415 **Table 4:** Fraction of the occupants' types in different scenarios

| | <i>Low Usage</i> | <i>Scenario I</i> | <i>High Usage</i> |
|-----------------------|------------------|-------------------|-------------------|
| <i>NTLU</i> | 23% | 16% | 10% |
| <i>NTMU</i> | 39% | 24% | 15% |
| <i>NTHU</i> | 33% | 53% | 65% |
| <i>TTCU</i> | 5% | 5% | 10% |
| <i>Peak Load (kW)</i> | 884 | 978 | 1,086 |

⁸ NTLU, NTMU, NTHU, TTCU

416

417 By changing the fraction of occupants, the energy demand profile for newly defined
 418 cases was predicted and provided as input to the energy model (see [Figure 6](#)). The boiler house
 419 equipment size remained similar to the *Scenario I*. After modeling these newly defined cases,
 420 the system performance under new conditions was determined. Comparing the percentage of
 421 the biomass boiler and thermal storage, which can cover the demand load of the community
 422 between the *Scenario I* and *High Usage Case* (see [Table 5](#)), shows that in the *High Usage*
 423 *Case* with 11% higher peak, the percentage coverage time by biomass boiler dropped by 1.1%.

424 **Table 5: Performance of the optimized system under new demand profile load**

| <i>Sensitivity Results</i> | | | |
|---|------------------|--------------------------|-------------------|
| Parameters | Low Usage | <i>Scenario I</i> | High Usage |
| Peak Heating Load (kW) | 884 | 978 | 1086 |
| Biomass Boiler (kW) | 477 | 477 | 477 |
| Auxiliary Boiler (kW) | 609 | 609 | 609 |
| Thermal Storage (m³) | 16.3 | 16.3 | 16.3 |
| Biomass Boiler Size Compared to the Peak Load (%) | 54 | 49 | 44 |
| Coverage Percentage by Biomass and Thermal Storage (%) | 97.8 | 95.0 | 93.9 |

425 **3.2. Scenario II (Newly Built Community):**

426 In the *Scenario II*, the weather file was changed, and the occupants' distribution was
 427 altered to the TTCU to represent the design criteria for newly built buildings. [Table 6](#) presents
 428 the optimal equipment sizes, resulting from the optimization of the boiler house for the
 429 *Scenario II*.

430 **Table 6: Scenario II: Optimization results**

| Parameters | Existing Situation | <i>Scenario II</i> |
|-------------------------------|---------------------------|---------------------------|
| Peak Heating Load (kW) | 1100 | 1189 |
| Biomass Boiler (kW) | 870 | 661 |
| Auxiliary Boiler (kW) | 1300 | 738 |

| | | |
|---|------|------|
| Thermal Storage (m³) | 50 | 32.8 |
| Biomass Boiler Size Compared to the Peak Load (%) | 79.1 | 56 |
| Coverage Percentage by Biomass and Thermal Storage (%) | -- | 98.8 |

431

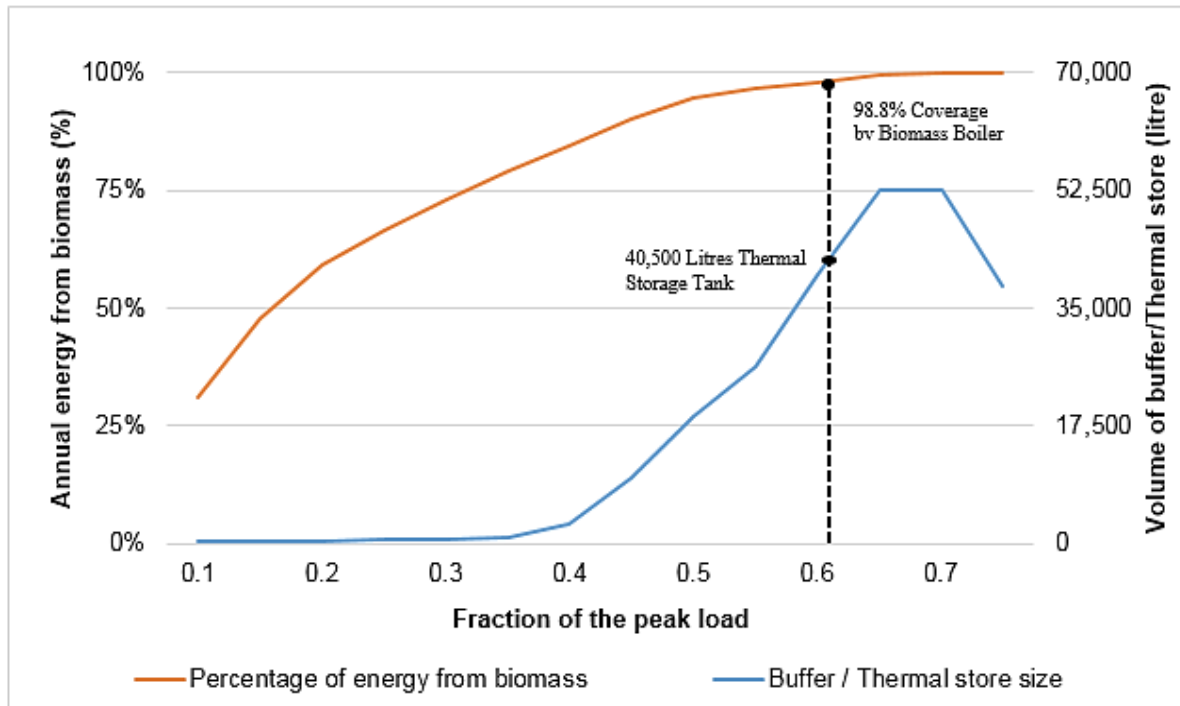


Figure 7: Optimal Equipment Size, Size of the biomass boiler as a percentage of a peak load for different annual % of energy from a biomass boiler

432

433

434

435

436 Similar to the *Scenario I*, the capacity of the boiler optimal size, biomass and auxiliary
 437 boiler, used less than 60% of their capacity to respond to the peak demand load. In order to find
 438 the optimal size of the equipment using the static optimized sizing tools such as Biomass Boiler
 439 Sizing Tool (version 6.8.2), primarily the same annual biomass energy coverage (98.8%) was
 440 determined. Using the same coverage percentage, the sizing tool suggests the biomass boiler
 441 with the capacity size of 62% of the peak load and 40.5 m³ thermal storage tank (refer to [Figure](#)
 442 [7](#)).

443

444

Table 7 presents the equipment size and cost associated with each design method.

445

Table 7: Comparison of the equipment size, cost for different design strategies

| Technology | Conventional | Static Optimization Tool | | Proposed Dynamic Optimization Process | |
|-----------------------------------|--------------|--------------------------|-------------------------|---------------------------------------|-------------------------|
| | | Size | Size Reduction * [%] | Size | Size Reduction * [%] |
| Biomass Boiler [kW] | 870 | 737 | 15.3 | 661 | 24.0% |
| Auxiliary Boiler [kW] | 1300 | 891 | 31.5 | 738 | 43.2% |
| Thermal Storage [m ³] | 50 | 40.5 | 19.0 | 32.5 | 35.0% |
| Cost [£] | 734,440 | 602,224 | 18.0 | 538,372 | 26.7% |

447

* Reductions calculated comparing with conventional method

448

449

450

451

452

453

454

455

456

457

458

459

460

Considering that only one boiler operates at a time, 98.8% coverage by biomass boiler was achieved using only thermal storage to balance between the generation and consumption loop. As shown in **Table 7**, this solution can reduce the size of both auxiliary and main biomass boilers into a fraction of their original size and, as a result, decrease the system heat loss while improving the district energy efficiency. The reduction in major equipment size of the district using the proposed dynamic optimization method caused a 196,068 £ or 26.7% drop only in the system initial investment cost. Also, knowing the fact that the efficiency of the biomass boiler is lower when operated partially, two scenarios could be assumed for a non-optimal size equipment: 1) the biomass boiler works at its full capacity all the time while keeping the generation efficiency at maximum value; this can result in generation of an excessive amount of heat, which eventually is accounted as loss, and 2) the boiler works at partial load only to meet the network demand. This decreases generation efficiency due to the boilers lower partial capacity efficiency [25]. In both scenarios, the overall efficiency of the system drops.

461

3.3. Impact of dynamic optimization in determining the operation period of the system

462

463

464

465

466

467

As mentioned earlier in **Section 1.1**, the main difference between the static and dynamic optimization is in dependency of the decision-making process with respect to time. In other words, dynamic optimization, by breaking the demand profile into smaller periods and determining a solution for each period, considers the effects of demand at the previous hour on the optimal solution. **Figure 8 (a)**, presents the charging/discharging profile of the thermal

468 storage over the 10 days period in November, obtained from the *Scenario I* and **Figure 8 (b)**
 469 represents the thermal energy storage mean temperature and the district demand load.

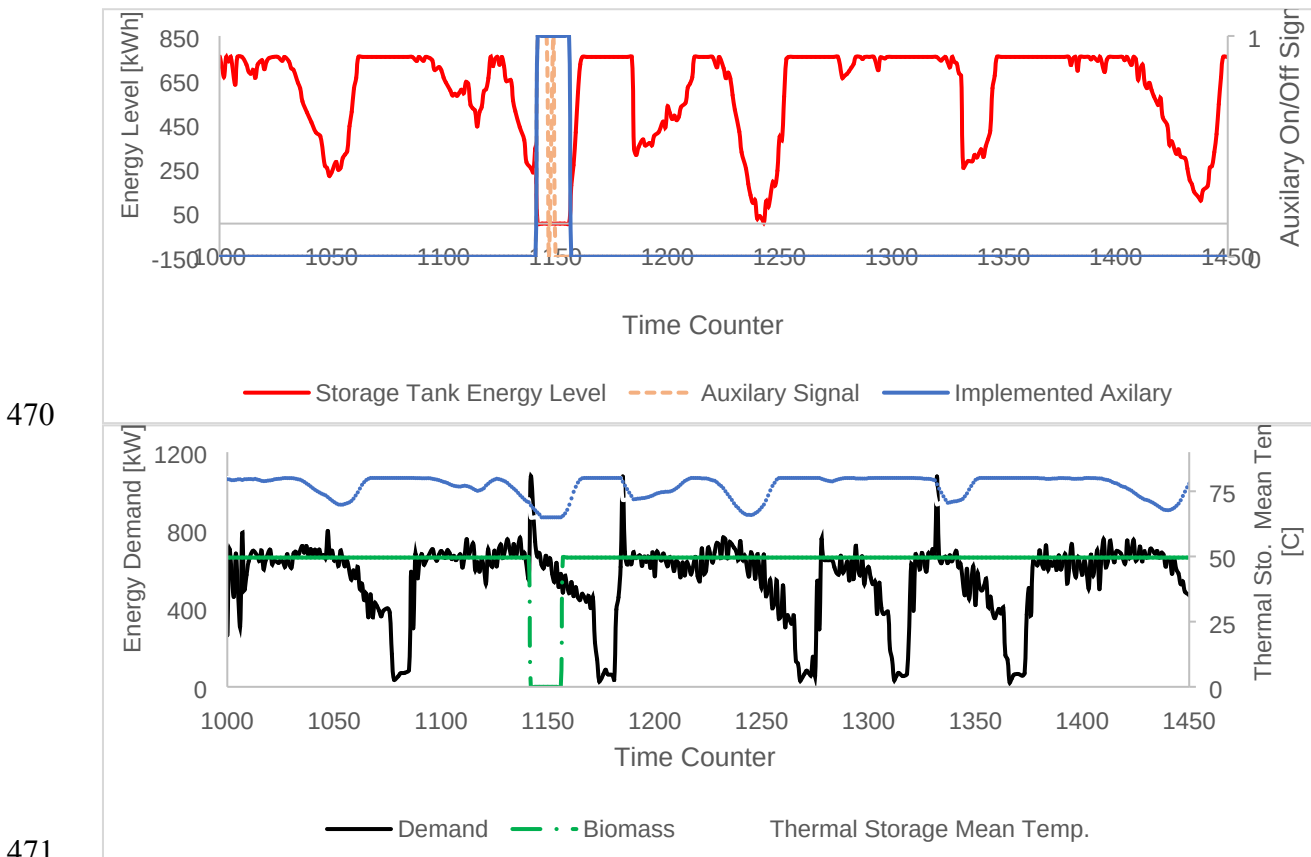


Figure 8: (a) Thermal storage energy level for a 10-day period in November; (b) Thermal storage temperature and district demand load for the same 10-days (Bottom)

475 In static optimization by only considering the peak demand in finding the optimal
 476 solution, the effects of the energy demand at previous hours on determining the optimal solution
 477 is neglected. On the other hand, in dynamic optimization, by considering the effects of the
 478 demand profile at a previous hour in determining the optimal solution can result in better
 479 utilizing of the thermal storage and lower size of the equipment. For instance, as presented in
 480 **Figure 8**, the response of the system to an identical demand varied based on the energy demand
 481 of the previous hours. In case of the first peak (shown in **Figure 8 (b)**), due to the high demand
 482 of the system prior to the peak, the thermal storage has been partially discharged, and as a result,
 483 the axillary energy is required to respond to the energy demand of the system. On the other

484 hand, due to lower demand of the network prior to the second and third peak, the thermal storage
485 is fully charged, and no auxiliary energy is required.

486 Apart from determining the optimal size of the equipment, the optimal performance of
487 the system could be determined from the proposed dynamic optimization method. As shown in
488 **Figure 8 (b)**, since the biomass boiler works constantly, the district demand load can be met
489 by a nominal size of the biomass boiler. However, when the demand load of the DHS is higher
490 than the capacity of the biomass boiler, the deficit energy is met from the thermal energy
491 storage. On the other hand, when the demand load drops, the surplus energy is stored in the
492 thermal energy storage and the energy storage level swiftly increases. In peak demand period,
493 the instantaneous auxiliary system (gas boiler in this case), along with thermal storage, provide
494 required energy demanded by the district network since the biomass boiler cannot provide
495 enough energy for the system. Using this strategy while running the biomass boiler constantly
496 at full capacity for the optimized sized system, step-wise charging/discharging the thermal
497 storage can eliminate the need for the auxiliary energy 98.8% of the time while maintaining the
498 system's maximum overall efficiency.

499 **4. Conclusion**

500 This study proposes a novel optimization process called dynamic optimization for
501 existing and newly built communities by coupling optimization and prediction using a
502 TRNSYS based energy simulation platform. Optimization performed to calculate the overall
503 size of major energy generation and storing equipment, and operational control strategy for the
504 community under different scenarios. In case of the existing community, **Scenario I**, comparing
505 the optimal equipment size with the existing non-optimal equipment sizes there exists a
506 considerable difference. The difference in equipment sizes (45% smaller biomass boiler, 53%
507 smaller auxiliary boiler and finally 67% smaller thermal storage size) between the existing
508 situation and the **Scenario I** is mainly due to the fact that the existing boiler house has been

509 designed based on the conventional methods. Beside from the drop in the initial cost of the
510 system (267,716 £ or 38.1%), the annual life cycle cost and CO₂ footprint of the district also
511 dropped by 79,056 £/year or 17.6% and 171.9 tons of CO₂ /year or 23% respectively. These
512 drops are due to the higher efficiency of the system operated at full capacity.

513 In case of a newly built district, *Scenario II*, three different design methods have been
514 used to size the equipment, conventional, static commercial optimization tool, and the
515 developed dynamic optimization process, and the respective results were compared. The results
516 indicate that initial cost of the system using the proposed dynamic optimization method could
517 drop by 26.7% compared with the conventional method while using the static optimization tool
518 could only result in 18% drop in the initial cost of the system. These facts emphasized the
519 importance of dynamic optimization of the system in order to achieve the real optimal solution.

520 **Acknowledgment**

521 The authors would like to express their gratitude to Concordia University for the support
522 through the Concordia Research Chair – Energy & Environment.

523
524

525 **References:**

- 526 1. Chu, S. and A. Majumdar, *Opportunities and challenges for a sustainable energy future.*
527 Nature, 2012. **488**: p. 294.
- 528 2. Christoff, P., *The promissory note: COP 21 and the Paris Climate Agreement.*
529 Environmental Politics, 2016. **25**(5): p. 765-787.
- 530 3. Zeng, J., J. Han, and G. Zhang, *Diameter optimization of district heating and cooling*
531 *piping network based on hourly load.* Applied Thermal Engineering, 2016.
532 **107**(Supplement C): p. 750-757.
- 533 4. Talebi, B., et al., *A Review of District Heating Systems: Modeling and Optimization.*
534 Frontiers in Built Environment, 2016. **2**(22).
- 535 5. Wang, W., X. Cheng, and X. Liang, *Optimization modeling of district heating networks*
536 *and calculation by the Newton method.* Applied Thermal Engineering, 2013. **61**(2): p.
537 163-170.
- 538 6. Wang, J., Z. Zhou, and J. Zhao, *A method for the steady-state thermal simulation of*
539 *district heating systems and model parameters calibration.* Energy Conversion and
540 Management, 2016. **120**: p. 294-305.
- 541 7. Chauhan, A. and R.P. Saini, *Discrete harmony search based size optimization of*
542 *Integrated Renewable Energy System for remote rural areas of Uttarakhand state in*
543 *India.* Renewable Energy, 2016. **94**: p. 587-604.

- 544 8. Mehleri, E.D., et al., *A mathematical programming approach for optimal design of*
545 *distributed energy systems at the neighbourhood level*. Energy, 2012. **44**(1): p. 96-104.
- 546 9. Olsthoorn, D., F. Haghghat, and P.A. Mirzaei, *Integration of storage and renewable*
547 *energy into district heating systems: A review of modelling and optimization*. Solar
548 Energy, 2016. **136**: p. 49-64.
- 549 10. Bordin, C., A. Gordini, and D. Vigo, *An optimization approach for district heating*
550 *strategic network design*. European Journal of Operational Research, 2016. **252**(1): p.
551 296-307.
- 552 11. Zhou, Z., et al., *Impacts of equipment off-design characteristics on the optimal design*
553 *and operation of combined cooling, heating and power systems*. Computers & Chemical
554 Engineering, 2013. **48**(Supplement C): p. 40-47.
- 555 12. Ameri, M. and Z. Besharati, *Optimal design and operation of district heating and*
556 *cooling networks with CCHP systems in a residential complex*. Energy and Buildings,
557 2016. **110**(Supplement C): p. 135-148.
- 558 13. Fang, T. and R. Lahdelma, *Genetic optimization of multi-plant heat production in*
559 *district heating networks*. Applied Energy, 2015. **159**(Supplement C): p. 610-619.
- 560 14. Razani, A.R. and I. Weidlich, *A genetic algorithm technique to optimize the*
561 *configuration of heat storage in DH networks*. 2016, 2016. **10**: p. 12.
- 562 15. Barberis, S., et al., *Thermo-economic analysis of the energy storage role in a real*
563 *polygenerative district*. Journal of Energy Storage, 2016. **5**(Supplement C): p. 187-202.
- 564 16. Vesterlund, M., A. Toffolo, and J. Dahl, *Optimization of multi-source complex district*
565 *heating network, a case study*. Energy, 2017. **126**(Supplement C): p. 53-63.
- 566 17. Wang, H., et al., *Optimization modeling for smart operation of multi-source district*
567 *heating with distributed variable-speed pumps*. Energy, 2017. **138**(Supplement C): p.
568 1247-1262.
- 569 18. Rivarolo, M., et al., *Design optimisation of smart poly-generation energy districts*
570 *through a model based approach*. Applied Thermal Engineering, 2016. **99**(Supplement
571 C): p. 291-301.
- 572 19. Magnier, L. and F. Haghghat, *Multiobjective optimization of building design using*
573 *TRNSYS simulations, genetic algorithm, and Artificial Neural Network*. Building and
574 Environment, 2010. **45**(3): p. 739-746.
- 575 20. Asadi, E., et al., *A multi-objective optimization model for building retrofit strategies*
576 *using TRNSYS simulations, GenOpt and MATLAB*. Building and Environment, 2012.
577 **56**: p. 370-378.
- 578 21. Campana, P.E., et al., *Optimization of a residential district with special consideration*
579 *on energy and water reliability*. Applied Energy, 2017. **194**(Supplement C): p. 751-764.
- 580 22. Schweiger, G., et al., *District heating and cooling systems – Framework for Modelica-*
581 *based simulation and dynamic optimization*. Energy, 2017. **137**(Supplement C): p. 566-
582 578.
- 583 23. Sameti, M. and F. Haghghat, *Optimization approaches in district heating and cooling*
584 *thermal network*. Energy and Buildings, 2017. **140**(Supplement C): p. 121-130.
- 585 24. Talebi, B., F. Haghghat, and P.A. Mirzaei, *Simplified model to predict the thermal*
586 *demand profile of districts*. Energy and Buildings, 2017. **145**: p. 213-225.
- 587 25. Camporeale, S.M., et al., *Part Load Performance and Operating Strategies of a Natural*
588 *Gas—Biomass Dual Fueled Microturbine for Combined Heat and Power Generation*.
589 Journal of Engineering for Gas Turbines and Power, 2015. **137**(12): p. 121401-121401-
590 13.
- 591 26. Talebi, Behrang, et al., *Validation of a community district energy system model using*
592 *field measured data*, Energy, 2018. **144**: p. 694-706.

593 27. R. Hitchin, U. Kingdom, K. E. Thomsen, and K. B. Wittchen, "Primary Energy Factors
594 and Members States Energy Regulations," no. 692447, 2010